

NSWC/DL TECHNICAL LIBRARY



2000345226

NSWC TR 88-250

926226

REFERENCE COPY

TECHNICAL LIBRARY

NAVAL SURFACE WARFARE CENTER

DAHLGREN, VA 22448-5020

DO NOT REMOVE FROM LIBRARY

## DETERMINATION OF CONSTITUTIVE MODEL CONSTANTS FROM CYLINDER IMPACT TESTS

BY T. J. HOLMQUIST AND G. R. JOHNSON  
(HONEYWELL, INC./ARMAMENT SYSTEMS DIVISION)

FOR NAVAL SURFACE WARFARE CENTER  
RESEARCH AND TECHNOLOGY DEPARTMENT

DECEMBER 1988

Approved for public release; distribution is unlimited.

NAUSWC-TR-88-250



**NAVAL SURFACE WARFARE CENTER**

Dahlgren, Virginia 22448-5000 • Silver Spring, Maryland 20903-5000

UNCLASSIFIED

SECURITY CLASSIFICATION OF THIS PAGE

## REPORT DOCUMENTATION PAGE

1a. REPORT SECURITY CLASSIFICATION <b>UNCLASSIFIED</b>			1b. RESTRICTIVE MARKINGS		
2a. SECURITY CLASSIFICATION AUTHORITY			3. DISTRIBUTION/AVAILABILITY OF REPORT  Approved for public release; distribution is unlimited.		
2b. DECLASSIFICATION/DOWNGRADING SCHEDULE					
4. PERFORMING ORGANIZATION REPORT NUMBER(S)			5. MONITORING ORGANIZATION REPORT NUMBER(S)  NSWC TR 88-250		
6a. NAME OF PERFORMING ORGANIZATION <b>Honeywell Inc. Armament Systems Division</b>		6b. OFFICE SYMBOL (If applicable)	7a. NAME OF MONITORING ORGANIZATION  Naval Surface Warfare Center		
6c. ADDRESS (City, State, and ZIP Code)  7225 Northland Drive Brooklyn Park, MN 55428			7b. ADDRESS (City, State, and ZIP Code)  10901 New Hampshire Avenue Silver Spring, MD 20903-5000		
8a. NAME OF FUNDING/SPONSORING ORGANIZATION  Naval Surface Warfare Center		8b. OFFICE SYMBOL (If applicable)  Code R12	9. PROCUREMENT INSTRUMENT IDENTIFICATION NUMBER  N60921-86-C-0249		
8c. ADDRESS (City, State, and ZIP Code)  10901 New Hampshire Avenue Silver Spring, MD 20903-5000			10. SOURCE OF FUNDING NOS.		
			PROGRAM ELEMENT NO.  62314N	PROJECT NO.  RJ14W21	TASK NO.  5
11. TITLE (Include Security Classification)  Determination of Constitutive Model Constants from Cylinder Impact Tests					
12. PERSONAL AUTHOR(S)  Holmquist, T. J. and Johnson, G. R.					
13a. TYPE OF REPORT  Final		13b. TIME COVERED FROM <u>11/86</u> TO <u>12/87</u>		14. DATE OF REPORT (Yr., Mo., Day)  1987, December	
15. PAGE COUNT  30					
16. SUPPLEMENTARY NOTATION					
17. COSATI CODES			18. SUBJECT TERMS (Continue on reverse if necessary and identify by block number)  Computer Codes Constitutive Models Material Response		
FIELD	GROUP	SUB. GR.			
12	01				
19. ABSTRACT (Continue on reverse if necessary and identify by block number)  This report describes and evaluates two computational strength models: The Johnson-Cook model and the Zerilli-Armstrong model. The models are compared to tension and torsion data, and to cylinder impact test data. Various techniques to obtain constants for the models, from cylinder impact test results, are also presented.					
20. DISTRIBUTION/AVAILABILITY OF ABSTRACT  <input type="checkbox"/> UNCLASSIFIED/UNLIMITED <input checked="" type="checkbox"/> SAME AS RPT. <input type="checkbox"/> DTIC USERS			21. ABSTRACT SECURITY CLASSIFICATION  UNCLASSIFIED		
22a. NAME OF RESPONSIBLE INDIVIDUAL  Paula Walter			22b. TELEPHONE NUMBER (Include Area Code)  (301) 394-2714		22c. OFFICE SYMBOL  Code R12

DD FORM 1473, 84 MAR

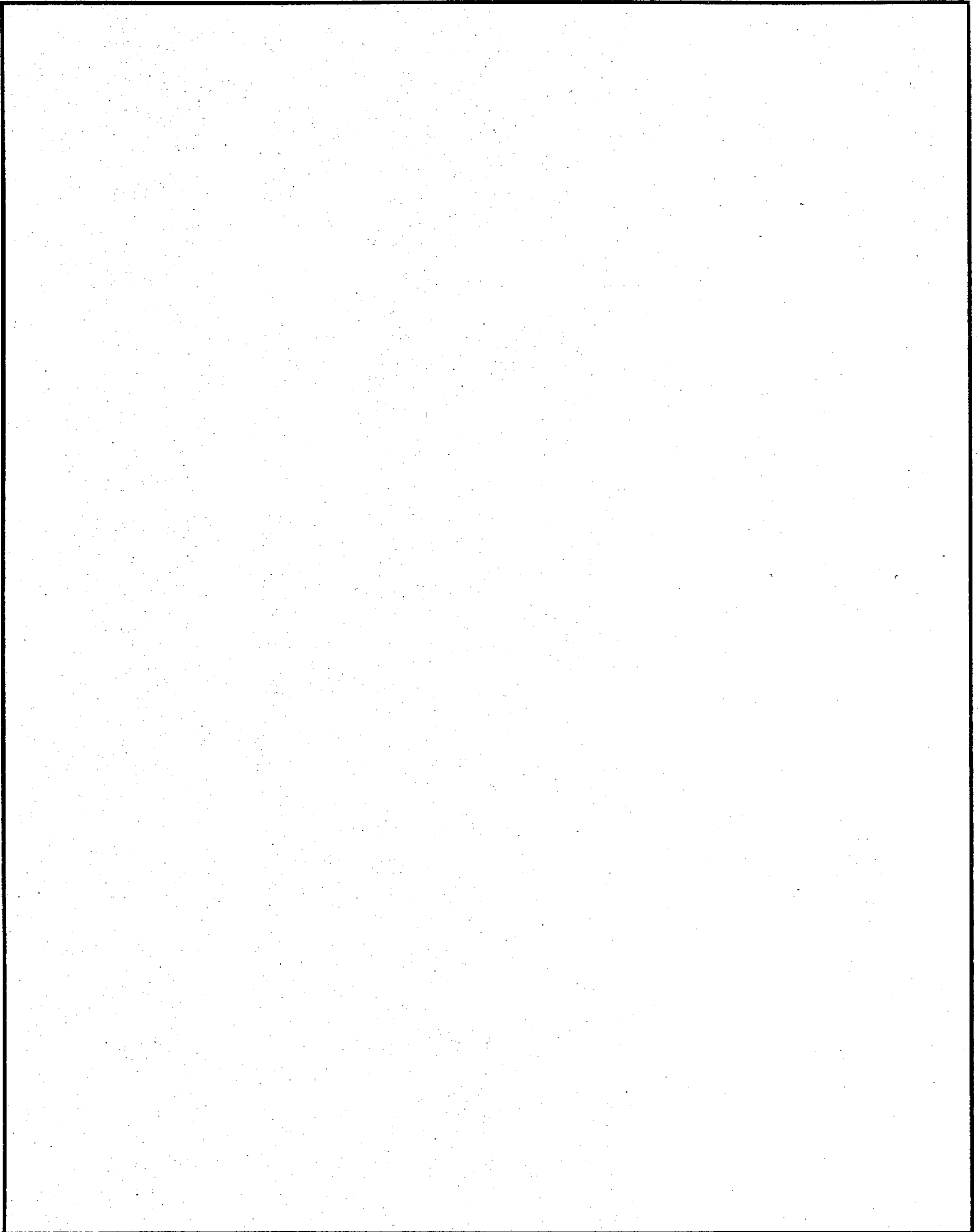
83 APR edition may be used until exhausted  
All other editions are obsolete

UNCLASSIFIED

SECURITY CLASSIFICATION OF THIS PAGE

**UNCLASSIFIED**

**SECURITY CLASSIFICATION OF THIS PAGE**



**UNCLASSIFIED**

**SECURITY CLASSIFICATION OF THIS PAGE**

## FOREWORD

This report was prepared by Honeywell Inc., Armament Systems Division, 7225 Northland Drive, Brooklyn Park, Minnesota 55428, for the White Oak Laboratory, Naval Surface Warfare Center (NSWC), 10901 New Hampshire Avenue, Silver Spring, Maryland 20903-5000, under contract N60921-86-C-0249.

This effort was conducted during the period from November 1986 to December 1987. The authors would like to thank Paula Walter, NSWC program manager, and Drs. Kibong Kim, Frank Zerilli, and Ronald Armstrong for helpful technical discussions during the course of this program.

Approved by:

A handwritten signature in cursive script, appearing to read "Kurt F. Mueller, Acting for".

DR. KURT F. MUELLER, Head  
Energetic Materials Division

**CONTENTS**

<u>Section</u>		<u>Page</u>
1	INTRODUCTION .....	1
2	THE JOHNSON-COOK AND ZERILLI-ARMSTRONG MODELS ...	3
3	COMPARISONS OF MODEL PREDICTIONS AND TEST DATA ..	7
4	DETERMINATION OF MODEL CONSTANTS FROM CYLINDER IMPACT TEST DATA .....	13
5	SUMMARY AND CONCLUSIONS .....	23
	REFERENCES .....	25
	DISTRIBUTION .....	(1)

## ILLUSTRATIONS

<u>Figure</u>		<u>Page</u>
1	ISOTHERMAL AND ADIABATIC STRESS-STRAIN RELATIONSHIPS FOR OFHC COPPER AND ARMCO IRON USING THE JOHNSON-COOK AND ZERILLI-ARMSTRONG MODELS ....	5
2	ADIABATIC STRESS-STRAIN RATE RELATIONSHIPS FOR OFHC COPPER AND ARMCO IRON USING THE JOHNSON-COOK AND ZERILLI-ARMSTRONG MODELS .....	6
3	COMPARISON OF JOHNSON-COOK AND ZERILLI-ARMSTRONG MODEL RESULTS WITH OFHC COPPER TEST DATA .....	8
4	COMPARISON OF JOHNSON-COOK AND ZERILLI-ARMSTRONG MODEL RESULTS WITH ARMCO IRON TEST DATA .....	9
5	COMPARISON OF CYLINDER IMPACT TEST RESULTS AND COMPUTED SHAPES FOR OFHC COPPER AND ARMCO IRON, USING THE JOHNSON-COOK AND ZERILLI-ARMSTRONG MODELS .....	10
6	DISTRIBUTION OF COMPUTED STRAINS OF OFHC COPPER AND ARMCO IRON CYLINDER IMPACT COMPUTATIONS, USING THE JOHNSON-COOK AND ZERILLI-ARMSTRONG MODEL .....	11
7	EXAMPLES OF CYLINDER IMPACT TEST RESULTS USED TO DETERMINE OFHC COPPER AND ARMCO IRON CONSTANTS FOR THE JOHNSON-COOK MODEL .....	14
8	COMPARISON OF ADIABATIC STRESS-STRAIN RELATIONSHIPS FOR VARIOUS OFHC COPPER AND ARMCO IRON CONSTANTS, USING THE JOHNSON-COOK MODEL .....	15
9	EXAMPLES OF CYLINDER IMPACT TEST RESULTS USED TO DETERMINE OFHC COPPER CONSTANTS FOR THE ZERILLI-ARMSTRONG MODEL .....	19
10	COMPARISON OF ADIABATIC STRESS-STRAIN RELATIONSHIPS FOR VARIOUS OFHC COPPER CONSTANTS, USING BOTH THE JOHNSON-COOK AND ZERILLI-ARMSTRONG MODELS .....	21

## SECTION 1

### INTRODUCTION

There are currently many different computer codes which can be used for computations of intense impulsive loading due to high velocity impact and/or explosive detonation. Although the current status of these codes is that they can now be used to perform meaningful computations, it is generally agreed that there is a need for improved strength and fracture models. There is also a need to develop efficient procedures to obtain constants for these models.

The work described in this report is focused on two computational strength models: The Johnson-Cook model<sup>1</sup> and the Zerilli-Armstrong model.<sup>2</sup> The report first describes the models and discusses relative comparisons. Then model predictions are compared with experimental data from tension/torsion tests and cylinder impact tests. This is followed by a discussion of how cylinder impact tests may be used to determine constants for these models. The report ends with a summary and conclusions.

## SECTION 2

## THE JOHNSON-COOK AND ZERILLI-ARMSTRONG MODELS

Most computational strength models express the equivalent (von Mises) tensile flow stress as a function of the equivalent plastic strain rate, temperature and/or pressure. For the Johnson-Cook model<sup>1</sup> the equivalent tensile flow stress is expressed as

$$\sigma = [A + B \epsilon^n][1 + C \ln \dot{\epsilon}^*][1 - T^{*m}] \quad (1)$$

where  $\epsilon$  is the equivalent plastic strain,  $\dot{\epsilon}^* = \dot{\epsilon}/\dot{\epsilon}_0$  is the dimensionless plastic strain rate for  $\dot{\epsilon}_0 = 1.0\text{s}^{-1}$ , and  $T^* = (T - T_{\text{room}})/(T_{\text{melt}} - T_{\text{room}})$  is the homologous temperature. The relationship is valid for  $0 \leq T^* \leq 1.0$ . The five material constants are A, B, n, C, and m.

The expression in the first set of brackets gives the stress as a function of strain for  $\dot{\epsilon}^* = 1.0$  and  $T^* = 0$ . The expressions in the second and third sets of brackets represent the effects of strain rate and temperature, respectively. At the melting temperature ( $T^* = 1.0$ ), the stress goes to zero for all strains and strain rates. The basic form of the model is readily adaptable to most computer codes, since it uses variables ( $\epsilon$ ,  $\dot{\epsilon}^*$ ,  $T^*$ ) which are available in the codes.

This model has some desirable features inasmuch as it is simple to implement, does not require excessive computing time or memory, can be used for a variety of metals, constants can be straightforwardly obtained from a limited number of laboratory tests, and the effects of the important variables are readily identifiable and separable.

The primary disadvantage of this model is that it is empirical and, therefore, has no sound physical basis. This means that exceptional care must be exercised when using it for extrapolated values of  $\epsilon$ ,  $\dot{\epsilon}^*$ , and  $T^*$ .

Some of the motivation and background for this model can be obtained from References 3 to 6, where an attempt was made to understand and simulate tests of large torsional strains over a range of strain rates.

Although various test techniques can be used to obtain constants for this model, the following has worked well.<sup>1</sup> First, the yield and strain hardening constants (A, B, n) are obtained from isothermal tension and torsion tests at relatively low strain rates ( $\dot{\epsilon}^* < 1.0$ ). Next, the strain rate constant, C, is determined from torsion tests at various strain rates, and tension tests (quasi-static and Hopkinson bar) at two strain rates. Finally, the thermal softening constant, m, is determined from Hopkinson bar tests at various temperatures.



Sometimes it is possible to obtain the yield and strain hardening constants (A, B, n) from cylinder impact tests. This will be more fully discussed in Section 4.

The Zerilli-Armstrong model is based on dislocation mechanics, and is, therefore, more physically based than the Johnson-Cook Model. The Zerilli-Armstrong model has two forms: one for face centered cubic (fcc) metals; and another for body centered cubic (bcc) metals.<sup>2</sup> The expression for fcc metals is

$$\sigma = C_0 + C_2 \varepsilon^{1/2} \exp(-C_3 T + C_4 T \ln \dot{\varepsilon}) \quad (2)$$

where  $\varepsilon$  is the equivalent plastic strain,  $\dot{\varepsilon}$  is the equivalent strain rate, and  $T$  is the absolute temperature. The four constants are  $C_0$ ,  $C_2$ ,  $C_3$ , and  $C_4$ . Here the initial yield stress,  $C_0$ , is independent of strain rate and temperature. Also, the stress does not necessarily go to zero at the melting temperature. Reference 2 provides a discussion of how  $C_0$  is affected by solute and grain size.

The expression for bcc metals is

$$\sigma = C_0 + C_1 \exp(-C_3 T + C_4 T \ln \dot{\varepsilon}) + C_5 \varepsilon^n \quad (3)$$

where the variables ( $\varepsilon$ ,  $\dot{\varepsilon}$ ,  $T$ ) are as defined for Equation (2) and six constants are  $C_0$ ,  $C_1$ ,  $C_3$ ,  $C_4$ ,  $C_5$ , and  $n$ . Here the initial yield stress is a function of  $C_0$ ,  $C_1$ ,  $C_3$ , and  $C_4$ . Again, the stress does not necessarily go to zero at the melting temperature.

It can be seen in Equation (2) that the strain, strain rate, and temperature effects are all coupled together for the fcc model. In Equation (3), however, the effect of strain hardening is separated from the coupled strain rate and temperature for the bcc model.

The fact that the Zerilli-Armstrong model is based on dislocation mechanics makes it preferable to the Johnson-Cook model. On the other hand, the more complex form of the Zerilli-Armstrong model appears to make it more difficult to obtain the appropriate constants.

Figure 1 shows a comparison of isothermal and adiabatic stress-strain relationships for the two models of interest. This is done for OFHC Copper (fcc) and Armco Iron (bcc). Constants for both models were obtained from essentially the same data base.<sup>1,2</sup>

For the OFHC copper, the Johnson-Cook model predicts higher adiabatic stresses at lower strains, and lower stresses at higher strains. For both the OFHC copper and the Armco iron, the Johnson-Cook model predicts less of a strain rate effect than does the Zerilli-Armstrong model. Generally, however, the adiabatic responses are similar for the two models.

Figure 2 shows the effect of strain rate for the two models. For the Armco Iron the Zerilli-Armstrong model shows a much stronger reliance on strain rate at the higher strain rates shown. This is consistent with torsion data for Armco IF Iron<sup>5</sup> and with trends predicted by other researchers.

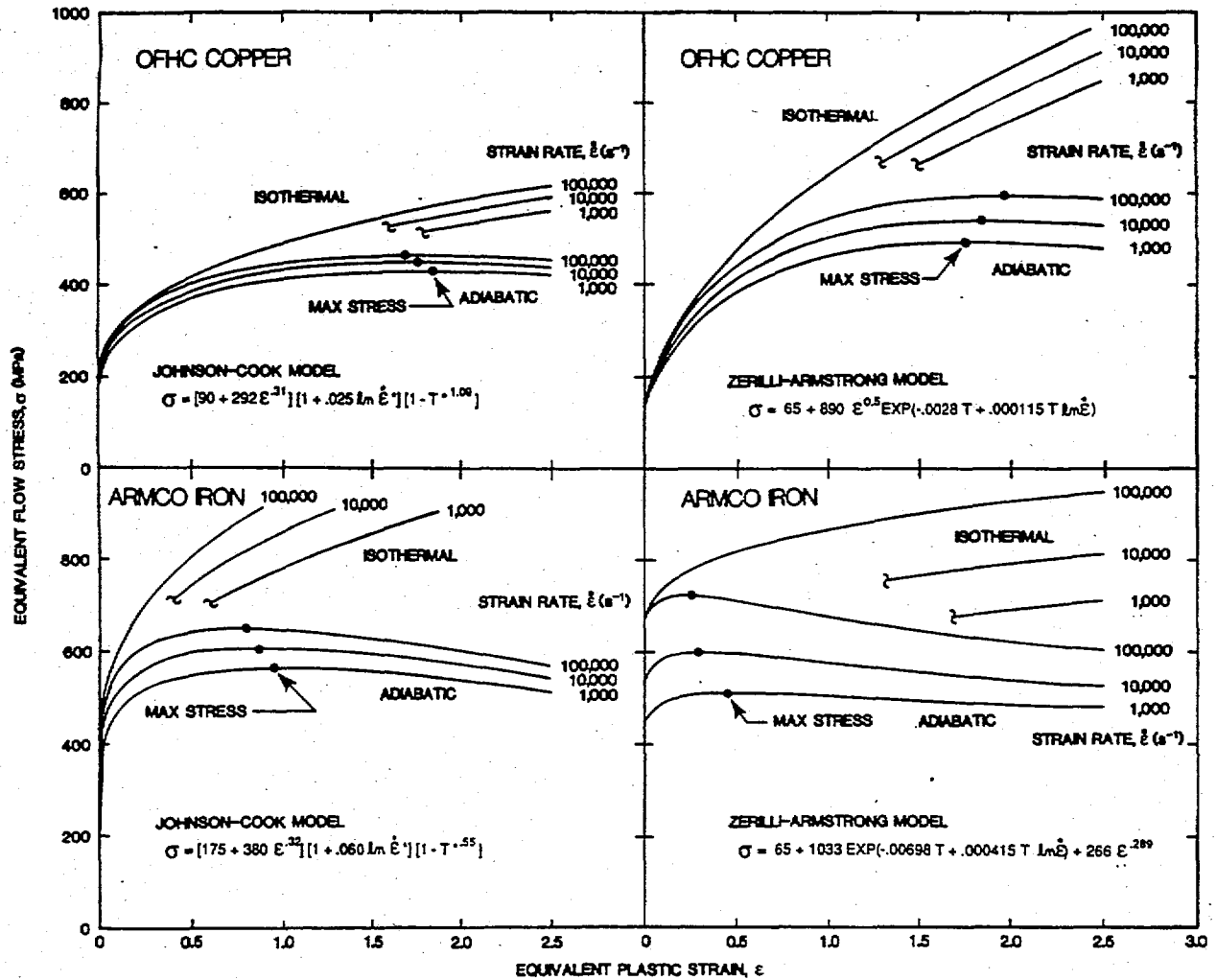


FIGURE 1. ISOTHERMAL AND ADIABATIC STRESS-STRAIN RELATIONSHIPS FOR OFHC COPPER AND ARMCO IRON USING THE JOHNSON-COOK AND ZERILLI-ARMSTRONG MODELS

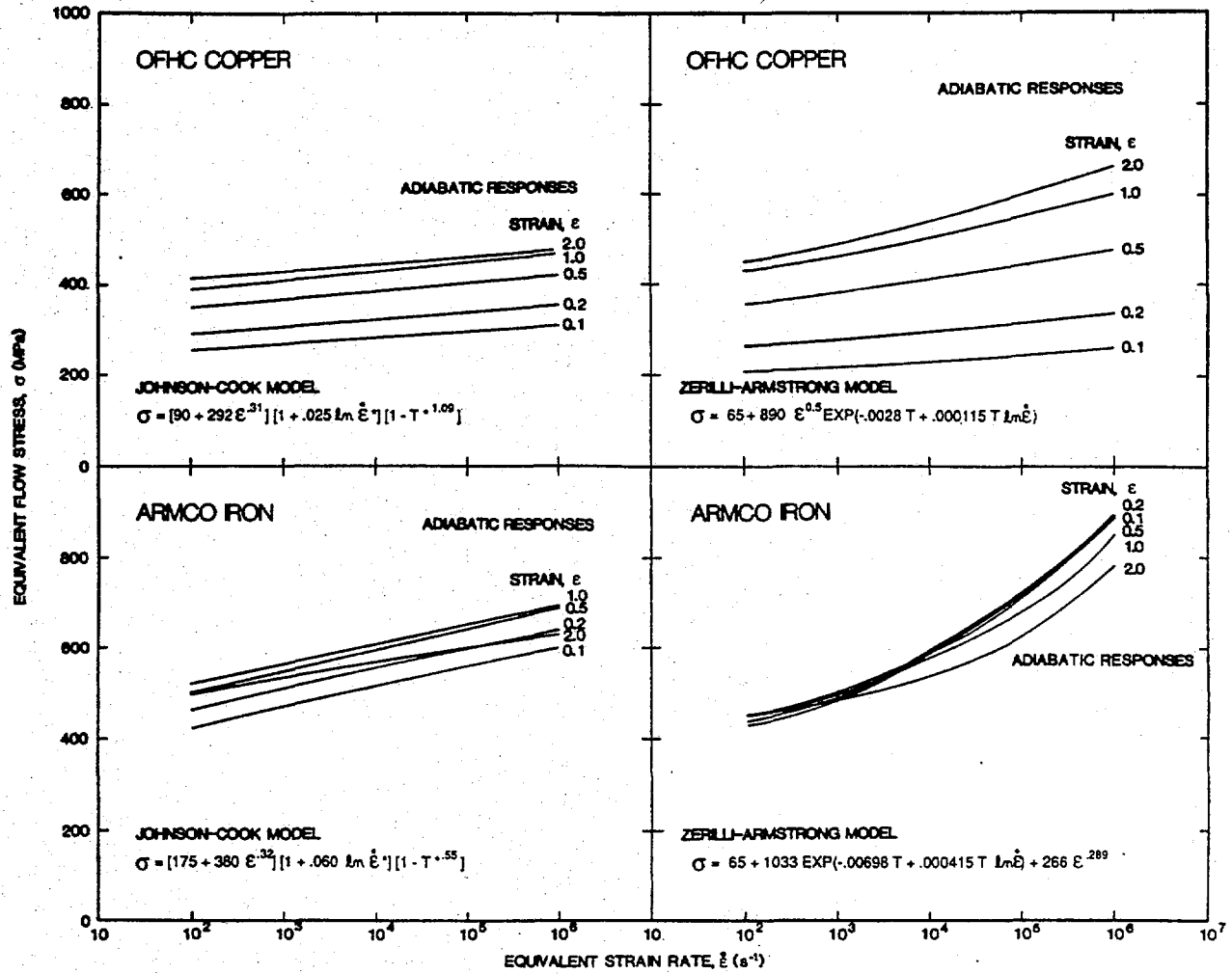


FIGURE 2. ADIABATIC STRESS-STRAIN RATE RELATIONSHIPS FOR OFHC COPPER AND ARMCO IRON USING THE JOHNSON-COOK AND ZERILLI-ARMSTRONG MODELS

## SECTION 3

## COMPARISON OF MODEL PREDICTIONS AND TEST DATA

An assessment of the models can be made by comparing the model predictions to experimental data. Figure 3 shows four comparisons for OFHC copper. The upper left portion of Figure 3 is for dynamic Hopkinson bar test data at room temperature, and the upper right portion is for similar data at an elevated temperature. It is assumed that the responses are adiabatic. There is relatively good agreement between the model predictions and the test data.

The lower portion of Figure 3 shows comparisons with quasi-static tension data and quasi-static torsion data. Here the responses are assumed to be isothermal. Both models tend to underpredict the strength in tension and overpredict the strength in torsion. This is due, in part to the fact that real materials do not always obey the von Mises flow rule,<sup>5</sup> which is an inherent part of most hydrocode computational algorithms. The von Mises flow rule states that the equivalent tensile stress and strain are  $\sigma = \sqrt{3}\tau$  and  $\epsilon = \gamma/\sqrt{3}$ , where  $\tau$  and  $\gamma$  are the shear stress and strain.

Figure 4 shows similar comparisons for Armco iron. Here again there is good general agreement with the Hopkinson bar data. Both models tend to underpredict the strength for the quasi-static tension and torsion data. The reason this occurs for the Johnson-Cook model is that the primary application is for higher strain rates, and the strain rate constant was therefore selected to give better correlation with the higher strain rate torsion data. This results in an underprediction of strength for lower strain rates ( $\dot{\epsilon}^* < 1.0$ ).

Another interesting evaluation is to compare the computed shapes of cylinder impacts onto a rigid surface, with actual test data, as shown in Figure 5. To quantify the degree of agreement between computed shapes and test data, an average error has been defined as

$$\bar{\Delta} = \frac{1}{3} \left[ \frac{|\Delta L|}{L} + \frac{|\Delta D|}{D} + \frac{|\Delta W|}{W} \right] \quad (4)$$

where L, D, and W are the deformed length, diameter, and bulge (diameter at  $0.2L_0$  from the deformed end) from the test results, and  $\Delta L$ ,  $\Delta D$ , and  $\Delta W$  are the differences between the computed and test results. It can be seen that both models give good general agreement, but that the Zerilli-Armstrong model gives better agreement.<sup>2</sup>

The maximum computed strains in Figure 5 fall within the range  $1.57 \leq \epsilon_{\max} \leq 2.04$ . The strain distributions in Figure 6, however, show that the overwhelming majority of the elements experience equivalent strains less than 0.6. Therefore, the comparisons in Figure 5 tend to reflect the accuracy of a model for relatively low strains ( $\epsilon < 0.6$ ), but do not necessarily provide a good indication for larger strains ( $\epsilon > 0.6$ ).

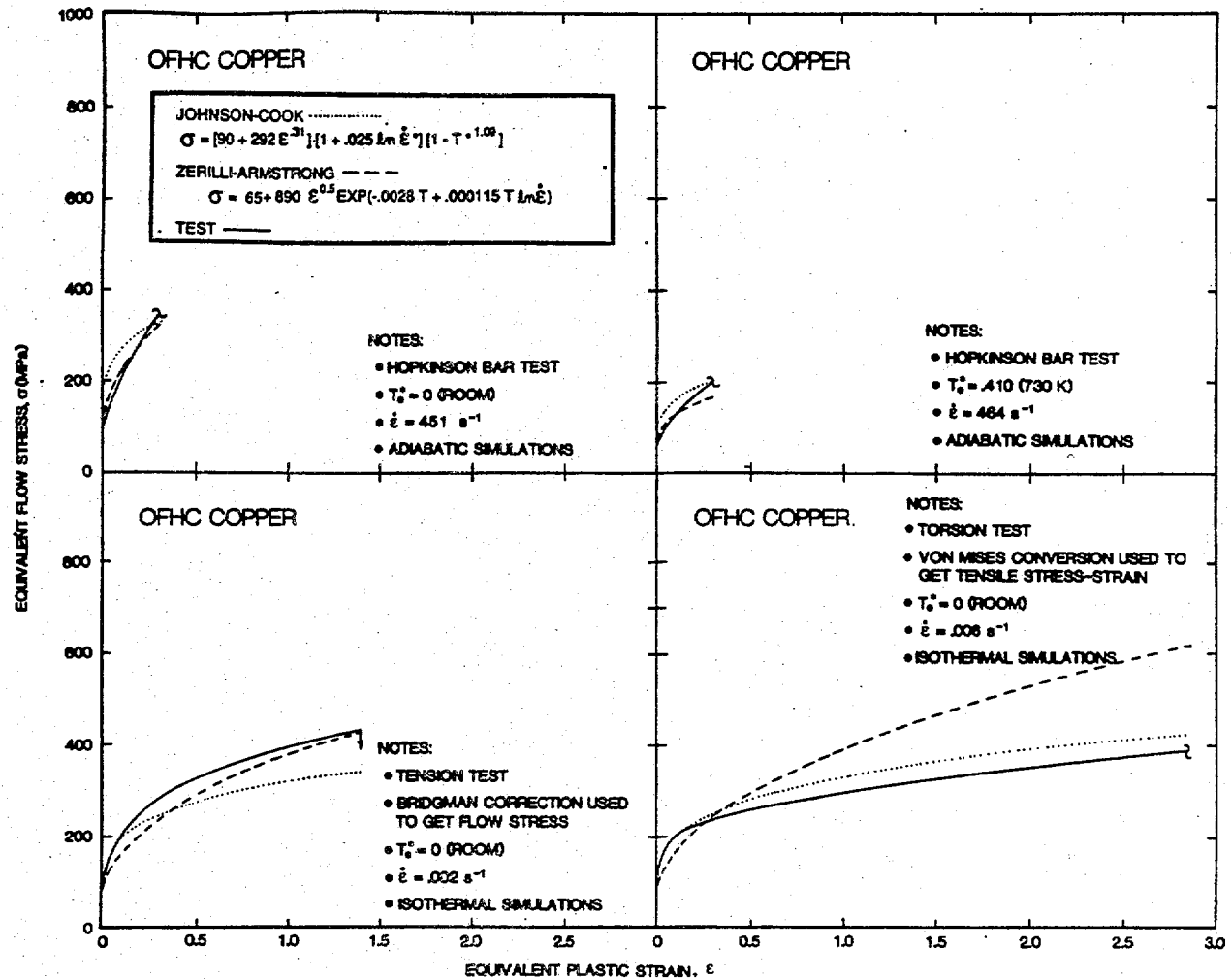


FIGURE 3. COMPARISON OF JOHNSON-COOK AND ZERILLI-ARMSTRONG MODEL RESULTS WITH OFHC COPPER TEST DATA

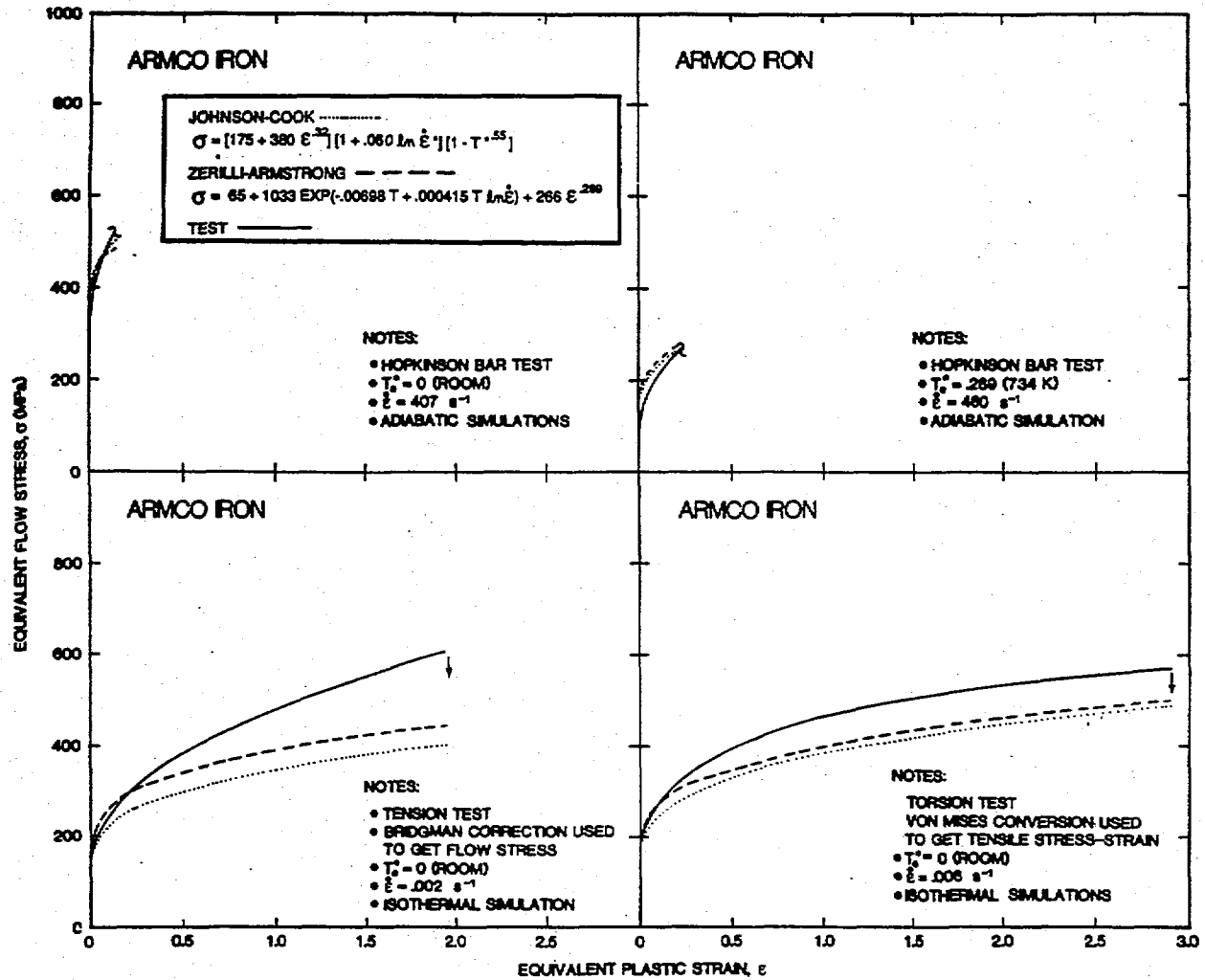


FIGURE 4. COMPARISON OF JOHNSON-COOK AND ZERILLI-ARMSTRONG MODEL RESULTS WITH ARMCO IRON TEST DATA

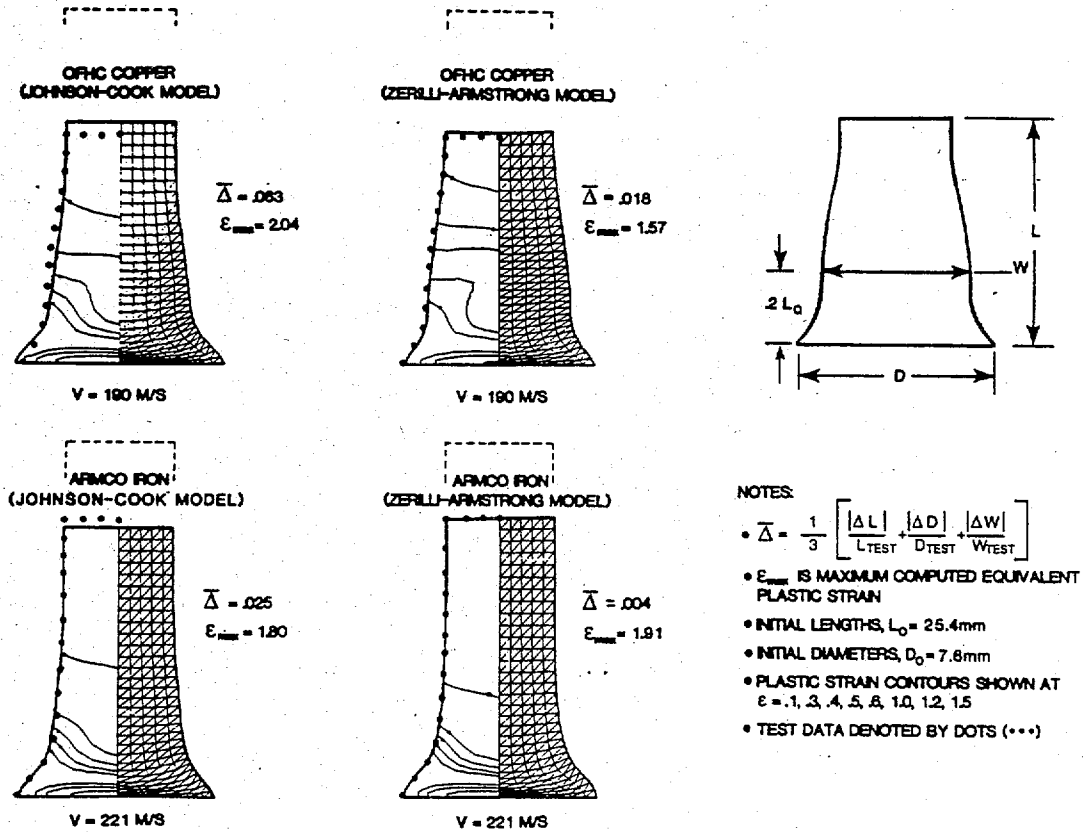


FIGURE 5. COMPARISON OF CYLINDER IMPACT TEST RESULTS AND COMPUTED SHAPES FOR OFHC COPPER AND ARMCO IRON, USING THE JOHNSON-COOK AND ZERILLI-ARMSTRONG MODELS

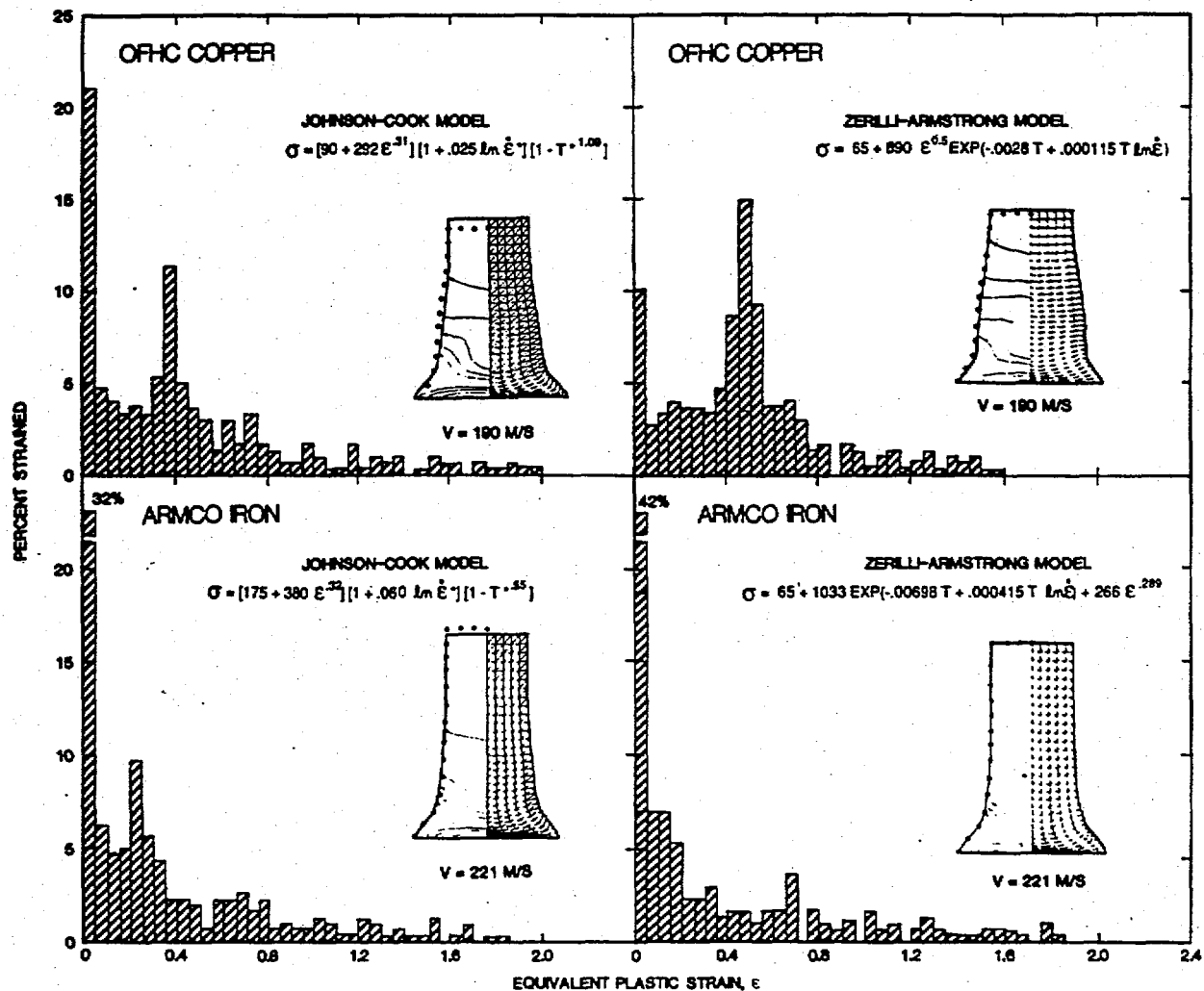


FIGURE 6. DISTRIBUTION OF COMPUTED STRAINS OF OFHC COPPER AND ARMCO IRON CYLINDER IMPACT COMPUTATIONS, USING THE JOHNSON-COOK AND ZERILLI-ARMSTRONG MODELS



## SECTION 4

DETERMINATION OF MODEL CONSTANTS FROM CYLINDER  
IMPACT TEST DATA

The preceding sections have attempted to define, understand, and evaluate the Johnson-Cook and Zerilli-Armstrong strength models. The constants for these models were obtained primarily from torsion tests at various strains rates, Hopkinson bar tests at various temperatures, and quasi-static tension tests. Performing these tests can often be time-consuming and/or expensive.

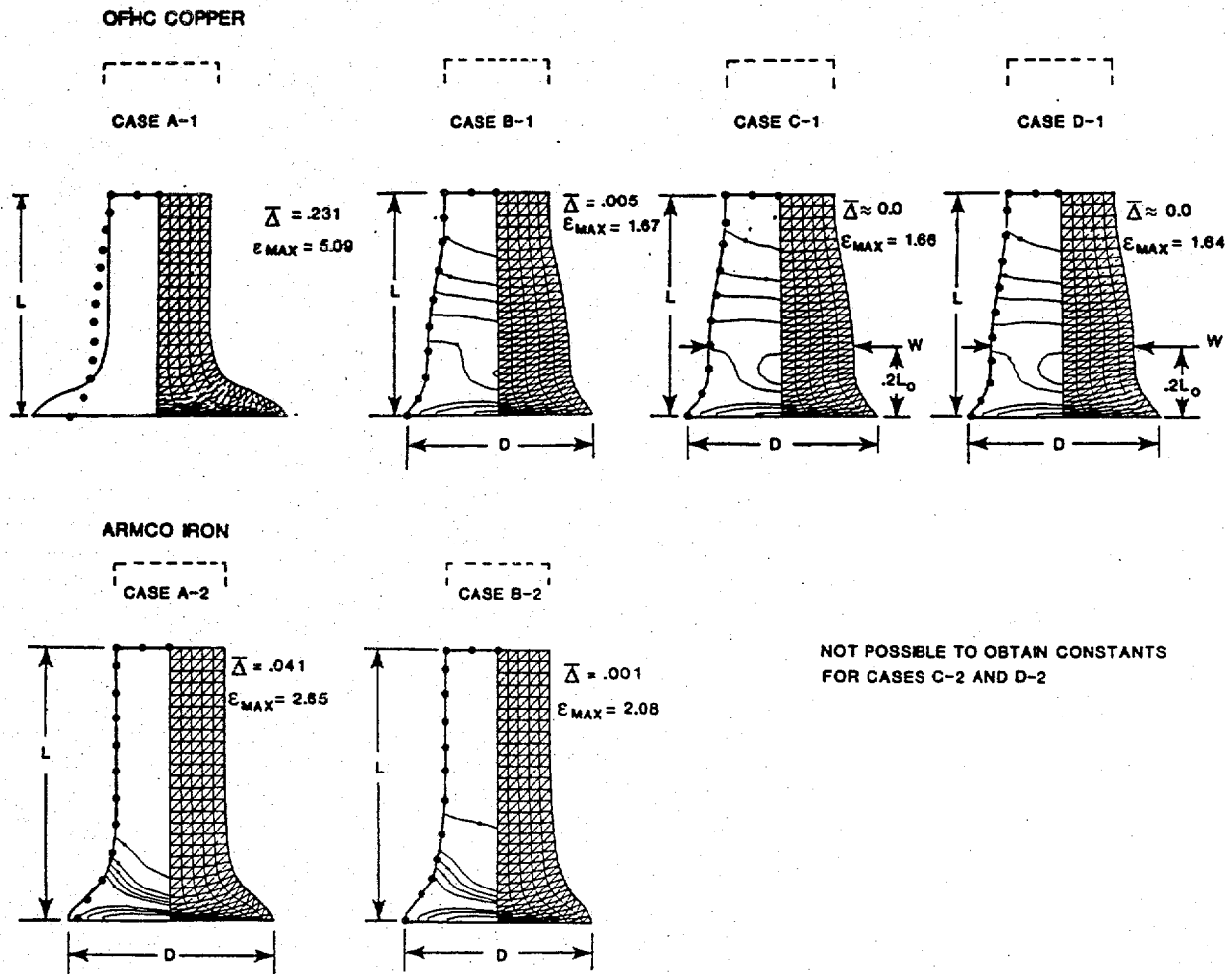
The cylinder impact test, on the other hand, is simple, inexpensive, and exhibits large strains, high strain rates, and elevated temperatures. Unfortunately, the strains, strain rates, temperatures, and stresses vary throughout the test specimen and throughout the duration of the test.

During the past years, there have been several attempts at defining dynamic flow stresses from cylinder impact test results.<sup>7-10</sup> Figure 7 shows how cylinder impact test data can be used to obtain constants for the Johnson-Cook Model. The test data are identical to those shown in Figure 5. The adiabatic stress-strain relationships are shown in Figure 8 and the strength constants are given in Table 1. The adiabatic stresses are shown only to the maximum strains attained in the computed results. Also included in Table 1 and Figure 8 are data from Reference 1 and Figure 1.

For Case A-1 the length,  $L$ , of the deformed cylinder (OFHC copper) is matched with the computational result. Because only one deformed dimension is matched, only one independent strength constant (representing a constant flow stress) can be obtained. It can be seen that there are significant discrepancies between the test and computational results at the deformed end of the cylinder.

Case B-1 allows for linear strain hardening. By matching both the deformed length,  $L$ , and the maximum diameter,  $D$ , it is possible to obtain the two constants for the linear hardening. Here the computed result is in good general agreement with the test result. If this model would be applied to larger strains than those experienced in the computed results of Case B-1, however, it would probably lead to excessively high stresses. It is well known that thermal softening tends to decrease the rate of strain hardening at large strains, as shown in Figure 1.

Cases C-1 and D-1 are based on the Johnson-Cook model of Equation (1). Although there are five constants in this model ( $A$ ,  $B$ ,  $n$ ,  $C$ ,  $m$ ), only the yield and strain hardening constants ( $A$ ,  $B$ ,  $n$ ) are determined from the test data. The strain rate constant,  $C$ , and the thermal softening constant,  $m$ , must be approximated or obtained from other sources. Because there are now three constants, it is possible to match three deformed dimensions: the length,  $L$ , the maximum diameter,  $D$ , and an intermediate diameter,  $W$ .



**NOTES:**

- OFHC COPPER CYLINDER ( $L_0 = 25.4\text{mm}$ ,  $D_0 = 7.6\text{mm}$ ,  $L_{TEST} = 16.2\text{mm}$ ,  $D_{TEST} = 13.5\text{mm}$ ,  $W_{TEST} = 10.1\text{mm}$ )
- ARMCO IRON CYLINDER ( $L_0 = 25.4\text{mm}$ ,  $D_0 = 7.6\text{mm}$ ,  $L_{TEST} = 19.8\text{mm}$ ,  $D_{TEST} = 13.7\text{mm}$ ,  $W_{TEST} = 8.6\text{mm}$ )
- IMPACT VELOCITIES = 190 m/s (OFHC COPPER) AND 221 m/s (ARMCO IRON)
- TEST RESULTS INDICATED BY DOTS • • •
- EQUIVALENT PLASTIC STRAIN CONTOURS SHOWN AT .1, .3, .4, .5, .6, 1.0, 1.2, 1.5
- ALL CASES COMPUTED WITH JOHNSON - COOK MODEL

**FIGURE 7. EXAMPLES OF CYLINDER IMPACT TEST RESULTS USED TO DETERMINE OFHC COPPER AND ARMCO IRON CONSTANTS FOR THE JOHNSON-COOK MODEL**

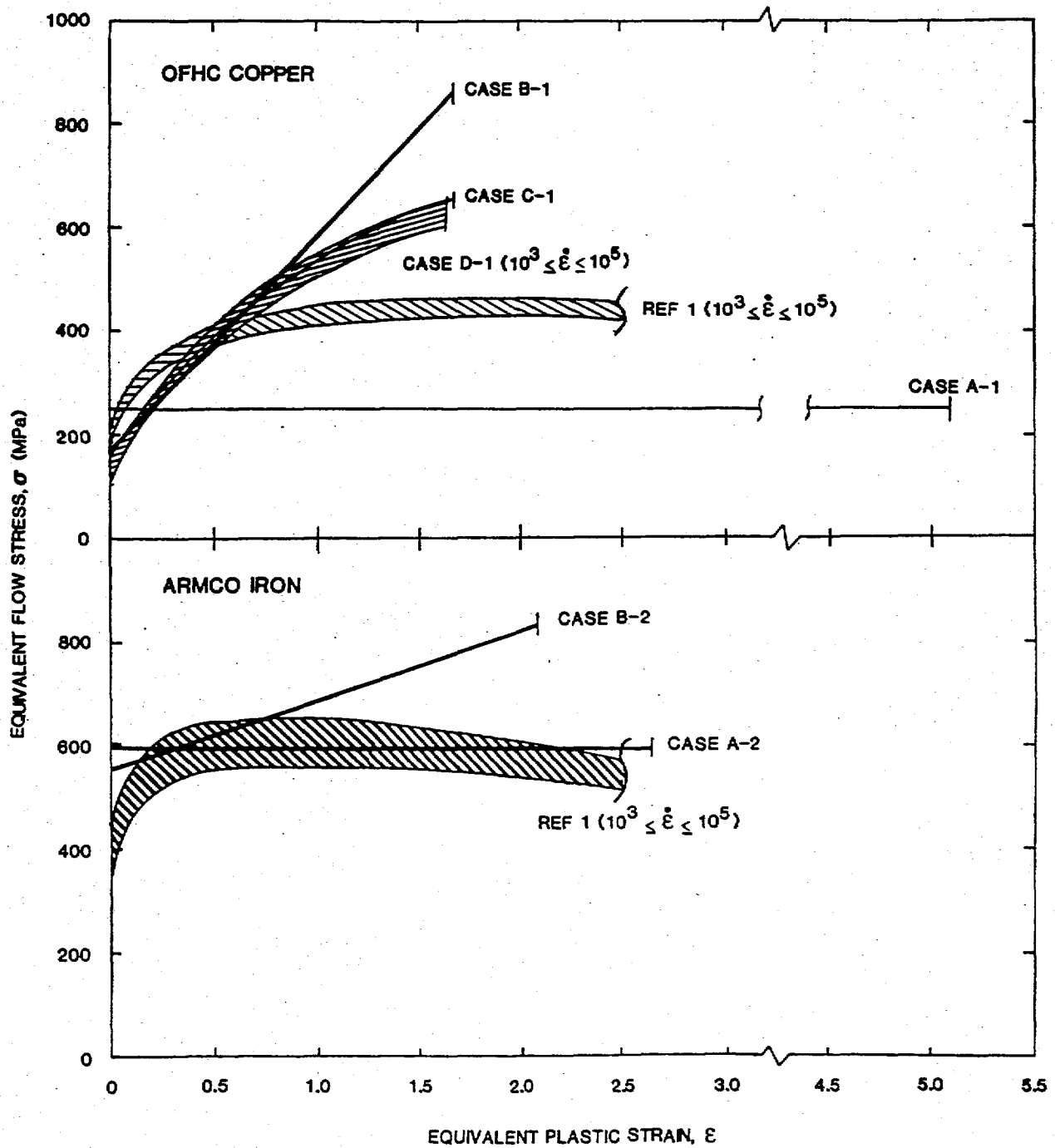


FIGURE 8. COMPARISON OF ADIABATIC STRESS-STRAIN RELATIONSHIPS FOR VARIOUS OFHC COPPER AND ARMCO IRON CONSTANTS, USING THE JOHNSON-COOK MODEL

**TABLE 1. OFHC COPPER AND ARMCO IRON CONSTANTS FOR THE JOHNSON-COOK MODEL, AS DETERMINED FROM CYLINDER IMPACT TEST RESULTS**

CONSTANTS FOR JOHNSON - COOK MODEL		OFHC COPPER				
$\sigma = [A+B\varepsilon^n] [1+C \ln \dot{\varepsilon}^*] [1-T^*{}^m]$		CASE A-1	CASE B-1	CASE C-1	CASE D-1	REF. 1
A	(Mpa)	250	157	118	98	90
B	(Mpa)	0.	425	484	368	292
n		-	1.00	.74	.70	.31
C		0.	0.	0.	.025	.025
m		-	-	1.00	1.09	1.09
		ARMCO IRON				
		CASE A-2	CASE B-2	CASE C-2	CASE D-2	REF.1
A	(Mpa)	593	555	NOT POSSIBLE TO		175
B	(Mpa)	0.	134	OBTAIN CONSTANTS		380
n		-	1.0	FOR CASES C-2		.32
C		0.	0.	AND D-2		.060
m		-	-			.55
$\dot{\varepsilon}^* = \dot{\varepsilon} / \dot{\varepsilon}_0$ FOR $\dot{\varepsilon}_0 = 1.0 \text{ S}^{-1}$ $T^* = (T - T_{\text{ROOM}}) / (T_{\text{MELT}} - T_{\text{ROOM}})$						

It should be noted that  $D$  and  $W$  are not totally independent of one another. For a given length,  $L$ ,  $W$  will tend to decrease as  $D$  increases. This is simply due to an approximate conservation of the volume of the cylinder.

Case C-1 is the result obtained if nothing is known about the strain rate or thermal softening characteristics of the material. Here, the strain rate constant is set to  $C = 0$  and the thermal softening is assumed to be linear, or  $m = 1.0$ . Case D-1 uses the previously determined strain rate and thermal softening constants from Reference 1 and Figure 1. Even though there is little apparent difference between Cases C-1 and D-1 for this problem, for some other problems (with wider ranges of strain rates and temperatures) the Case D-1 constants will probably provide better results.

Looking at Figure 8, it can be seen that there are significant discrepancies in the various adiabatic stress-strain relationships, especially at the larger strains. Yet, with the exception of Case A-1, they all provide a generally good correlation with the test data. The reason for this situation is provided in the distribution of strain, as shown previously in the upper-left portion of Figure 6. Although some of the elements experience an equivalent plastic strain as high as 2.04, most of the elements experience strains less than 0.6. Looking back to this specific range of strains in Figure 8, there is good general agreement (except for Case A-1) between the various adiabatic stress-strain relationships. Therefore, because the various models essentially agree with one another in this relatively narrow band of strain, it would be expected that they would give similar results for computed solutions whose strains fall within this narrow band.

In the lower portion of Figure 7, the same approach was attempted for the Armco iron. For Case A-2 only the length,  $L$ , was matched, giving a constant flow stress. For Case B-2 the length,  $L$ , and diameter,  $D$ , were matched using linear strain hardening. The resulting adiabatic flow stresses are shown in Figure 8. There is clearly less strain hardening in the Armco iron than in the OFHC copper.

For Cases C-2 and D-2, however, it was not possible to match all three dimensions ( $L$ ,  $D$ ,  $W$ ) by varying the yield and strain hardening constants ( $A$ ,  $B$ ,  $n$ ). This is probably due to the fact that there is less strain hardening in the Armco iron (when compared to the OFHC copper), and therefore less of a bulge,  $W$ . It appears that it simply is not possible to extract strain-hardening constants for test data which exhibit very little strain hardening. Also, the empirical form of Equation (1) may not be well suited to accurately represent the Armco iron.

For the Johnson-Cook model, it appears that it is possible to obtain the yield and strain hardening constants ( $A$ ,  $B$ ,  $n$ ) for some materials, but not for all materials. This is probably dependent on the degree of strain hardening in the material. The strain rate and thermal softening constants ( $C$ ,  $m$ ) must be approximated or obtained from other sources. It is also not desirable to extrapolate the use of the model to larger strains than experienced in the cylinder impact test.

Looking at the Zerilli-Armstrong models in Equations (2) and (3), it can be seen that four constants are needed for fcc metals (such as OFHC copper) and six constants are needed for bcc metals (such as Armco Iron). Based on previous experience with the Johnson-Cook model, only two or three constants can be obtained from the shape of the deformed cylinder.

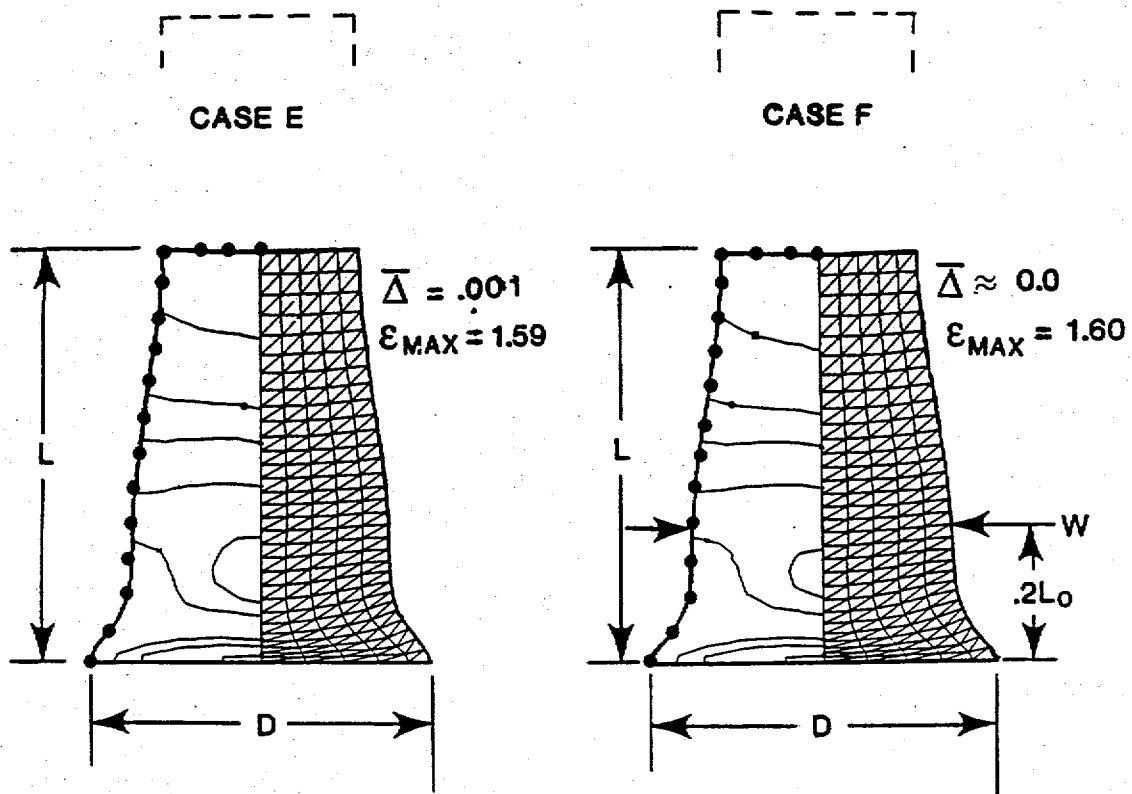
Looking again at Equation (2) for fcc metals, it would appear that the first two constants ( $C_0$ ,  $C_2$ ) could be obtained from the cylinder impact test data, if the strain rate and thermal softening constants ( $C_3$ ,  $C_4$ ) could be approximated or obtained from other sources. These results are shown as Case E in Figure 9. The length,  $L$ , and diameter,  $D$ , have been matched exactly, and the resulting bulge,  $W$ , is very close to that of the test data. The new constants, ( $C_0$  and  $C_2$ ) were obtained in conjunction with the previous values of  $C_3$  and  $C_4$ , as taken from Reference 2.

Another approach is to obtain the yield stress,  $C_0$ , from another source, and then solve for  $C_2$ ,  $C_3$ , and  $C_4$  by matching the three deformed dimensions ( $L$ ,  $D$ ,  $W$ ). The yield stress in Equation (2) is independent of both the strain rate and the temperature, and can, therefore, be easily determined from simple tension tests and/or handbook data. The results of this approach are shown as Case F in Figure 9, where the new constants ( $C_2$ ,  $C_3$ ,  $C_4$ ) were obtained for the previous value of  $C_0$ , as taken from Reference 2. A summary of the constants for Cases E and F is given in Table 2.

It is interesting to compare the adiabatic stress-strain relationships of Case D-1 (Johnson-Cook) and Case F (Zerilli-Armstrong), because both of these cases give a perfect fit ( $\Delta \approx 0$ ) to the test data. These two cases, along with three other cases, are shown in Figure 10. As expected, the responses of Cases D-1 and F are very similar at smaller strains ( $\epsilon < 0.6$ ). They are also in good general agreement at larger strains. Case E, where only two constants were determined for the Zerilli-Armstrong model, is also shown in Figure 10.

It should be noted that the actual values of the constants in Cases E and F may or may not be physically realistic. For these cases, the constants are selected only to match the deformed shape of the cylinder. The other two curves are from Reference 1, which presents the initial Johnson-Cook model and data, and from Reference 2, which presents the initial Zerilli-Armstrong model and data.

An attempt was made to determine three constants ( $C_0$ ,  $C_5$ ,  $n$ ) from the Zerilli-Armstrong model of Equation (3) for Armco iron, using the reported values<sup>2</sup> of the other three constants ( $C_2$ ,  $C_3$ ,  $C_4$ ). As was the case with the Johnson-Cook model (Cases C-2 and D-2), however, it was not possible to match all three dimensions ( $L$ ,  $D$ ,  $W$ ) of the test results.

**NOTES:**

- OFHC COPPER CYLINDER ( $L_0 = 25.4\text{mm}$ ,  $D_0 = 7.6\text{mm}$ ,  
 $L_{TEST} = 16.2\text{mm}$ ,  $D_{TEST} = 13.5\text{mm}$ ,  $W_{TEST} = 10.1\text{mm}$ )
- IMPACT VELOCITY = 190 M/S
- TEST RESULTS INDICATED BY DOTS • • •
- EQUIVALENT PLASTIC STRAIN CONTOURS SHOWN AT  
 .1, .3, .4, .5, .6, 1.0, 1.2, 1.5
- BOTH CASES COMPUTED WITH ZERILLI-ARMSTRONG MODEL

**FIGURE 9. EXAMPLES OF CYLINDER IMPACT TEST RESULTS USED TO DETERMINE OFHC COPPER CONSTANTS FOR THE ZERILLI-ARMSTRONG MODEL**

TABLE 2. OFHC COPPER CONSTANTS FOR THE ZERILLI-ARMSTRONG MODEL, AS DETERMINED FROM CYLINDER IMPACT TEST RESULTS

CONSTANTS FOR ZERILLI-ARMSTRONG FACE CENTERED CUBIC MODEL $\sigma = C_0 + C_2 \dot{\epsilon}^{0.5} \exp(-C_3 T + C_4 T \ln \dot{\epsilon})$		OFHC COPPER		
		CASE E	CASE F	REF 2
C <sub>0</sub>	(Mpa)	38	65	65
C <sub>2</sub>	(Mpa)	903	546	890
C <sub>3</sub>	(°K <sup>-1</sup> )	.0028	.0025	.0028
C <sub>4</sub>	(°K <sup>-1</sup> )	.000115	.000199	.000115



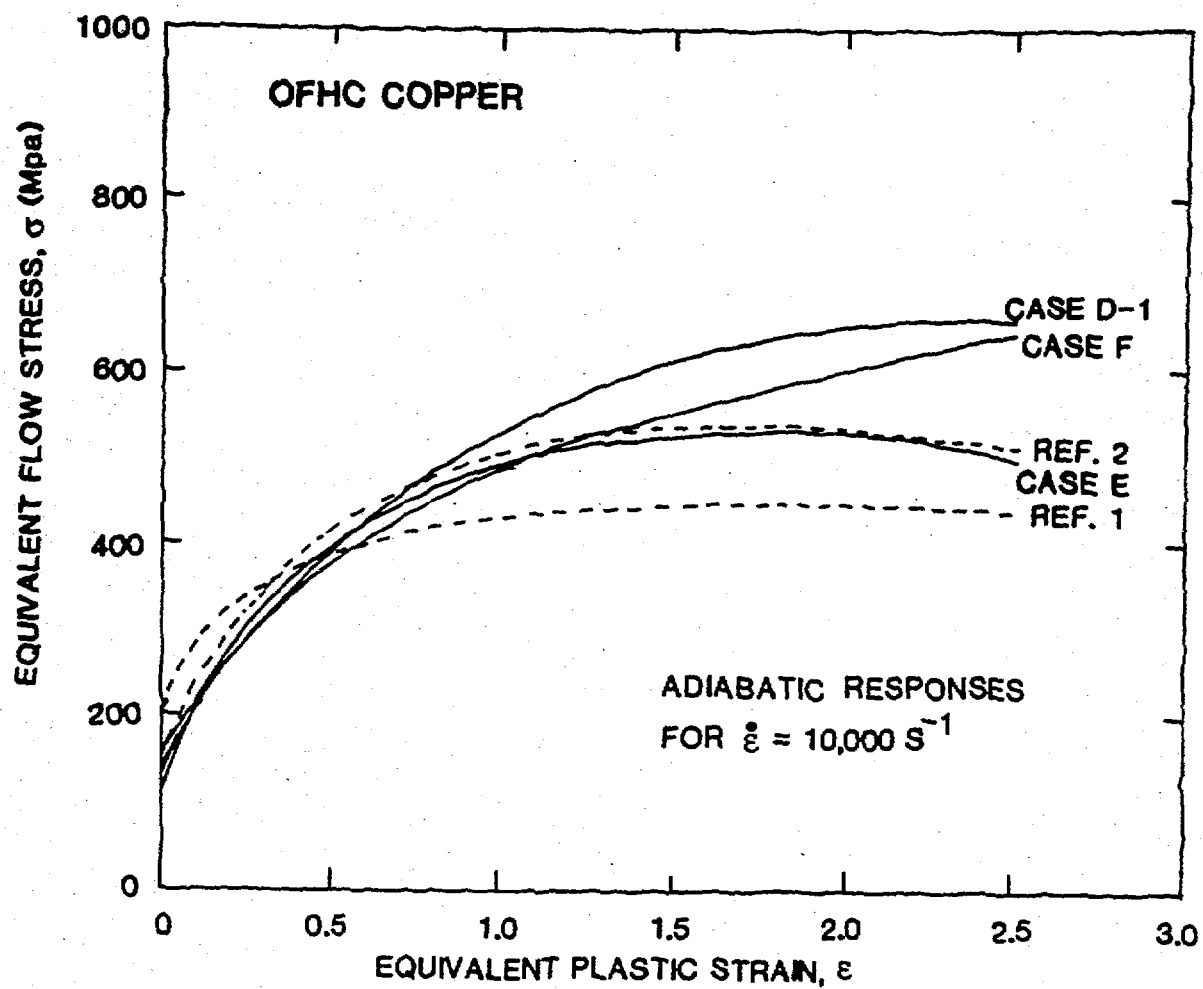


FIGURE 10. COMPARISON OF ADIABATIC STRESS-STRAIN RELATIONSHIPS FOR VARIOUS OFHC COPPER CONSTANTS, USING BOTH THE JOHNSON-COOK AND ZERILLI-ARMSTRONG MODELS

## SECTION 5

### SUMMARY AND CONCLUSIONS

This report has attempted to describe and evaluate two computational strength models, and to determine how constants might be obtained from cylinder impact test results. Some conclusions are as follows:

- The Zerilli-Armstrong model is more physically based and provides better agreement with the cylinder impact test data.
- The Johnson-Cook model has a more simple form which allows the constants to be obtained in a more straightforward manner.
- Both models show generally good agreement with Hopkinson bar test data at relatively low strains.
- Both models show discrepancies with quasi-static tension and torsion data at large strains. This is probably due to the inadequacy of the von Mises flow rule at large strains.
- Cylinder impact test results can be used to determine two or three constants for either the Johnson-Cook model or the Zerilli-Armstrong model. The other constants must be estimated or obtained from other sources.
- When the length and diameter of the cylinder impact test data are matched by determining two constants, the resulting bulge is generally in close agreement because the cylinder tends to conserve volume.
- The accuracy of either model has not been evaluated for the combination of large strains ( $\epsilon > 0.6$ ) and high-strain rates ( $\dot{\epsilon} > 10^3$ ). In unpublished work not performed in this contract, however, the Johnson-Cook model has been used to give good overall predictions of Explosive Formed Penetrators for both OFHC copper and Armco iron. Here, most of the material is strained to a much greater extent than it is in the cylinder-impact tests.

## REFERENCES

1. Johnson, G. R. and Cook, W. H., "A Constitutive Model and Data for Metals Subjected to Large Strains, High Strain Rates and High Temperatures," Proceedings of Seventh International Symposium on Ballistics, The Hague, The Netherlands, Apr 1983.
2. Zerilli, F. J. and Armstrong, R. W., "Dislocation-Mechanics-Based Constitutive Relations for Material Dynamics Calculations," Journal of Applied Physics, Vol. 61, No. 5, Mar 1987.
3. Linkholm, U. S., Nagy, A., Johnson, G. R., and Hoegfeldt, J. M., "Large Strain, High Strain Rate Testing of Copper," Journal of Engineering Materials and Technology, ASME, Vol. 102, Oct 1980.
4. Johnson, G. R., "Dynamic Analysis of a Torsion Test Specimen Including Heat Conduction and Plastic Flow," Journal of Engineering Materials and Technology, ASME, Vol. 103, Jul 1981.
5. Johnson, G. R., Hoegfeldt, J. M., Lindholm, U. S., and Nagy, A., "Response of Various Metals to Large Torsional Strains Over a Large Range of Strain Rates--Part 1: Ductile Metals," Journal of Engineering Materials and Technology, ASME, Vol. 105, Jan 1983.
6. Johnson, G. R., Hoegfeldt, J. M., Lindholm, U. S., and Nagy, A., "Response of Various Metals to Large Torsional Strains Over a Large Range of Strain Rates--Part 2: Less Ductile Metals," Journal of Engineering Materials and Technology, ASME, Vol. 105, Jan 1983.
7. Taylor, G. I., "The Use of Flat-Ended Projectiles for Determining the Dynamic Yield Stress," Proceedings of Royal Society, 1948.
8. Wilkins, M. L. and Guinan, M. W., "Impact of Cylinders on a Rigid Body," Journal of Applied Physics, Vol. 44, No. 3, 1973.
9. Erlich, D. C. and Chartegnac, P., "Determination of Dynamic Flow Curve of Metals at Ambient and Elevated Temperatures by Rod Impact Techniques," Proceedings of International Conference on Mechanical and Physical Behavior of Materials Under Dynamic Loading, Paris, France, Sep 1985.
10. Holmquist, T. J. and Johnson, G. R., "A Direct Method to Obtain Constitutive Model Constants from Cylinder Impact Test Results," Proceedings of Work-In-Progress at Army Symposium on Solid Mechanics, MTL MS 86-3, West Point, NY, Oct 1986.

## DISTRIBUTION

	<u>Copies</u>		<u>Copies</u>
Chief of Naval Operations Attn: Technical Library Department of the Navy Washington, DC 20350	1	Commanding Officer Naval Ordnance Station Attn: Technical Library Indian Head, MD 20640	1
Office of Naval Technology Attn: OCNR-23	1	Commanding Officer Naval Ship Weapons Systems Engineering Station	
OCNR-232	1	Port Hueneme, CA 93043	1
OCNR-213	1		
800 North Quincy Street Ballston Center Towers #1 Room 503 Arlington, VA 22217-5000		Commanding Officer Naval Undersea Warfare Engineering Station Keyport, WA 98345	1
Commander Naval Ocean Systems Center Attn: Technical Library San Diego, CA 92152	1	Commander Naval Weapons Evaluation Facility Kirtland Air Force Base Albuquerque, NM 87117	1
Defense Technical Information Center Cameron Station Alexandria, VA 22314	12	Commander Naval Underwater Systems Center Attn: Technical Library Newport, RI 02840	1
Office of Naval Research Attn: Technical Library 800 North Quincy Street Arlington, VA 22217	1	Director Defense Advanced Research Projects Agency Attn: Library Naval Technology Office 1400 Wilson Boulevard Arlington, VA 22209	1 1
Sandia National Laboratories Attn: Technical Library Albuquerque, NM 87185	1	Commander Naval Weapons Center Attn: Technical Library Code 3917 China Lake, CA 93555	1 1
Director Defense Nuclear Agency Attn: Technical Library Washington, DC 20305	1		
Commanding Officer Naval Coastal Systems Center Attn: Technical Library Panama City, FL 32407	1		

## DISTRIBUTION (Cont.)

	<u>Copies</u>		<u>Copies</u>
Commander		Internal Distribution:	
Naval Air Systems Command		E231	2
Attn: Technical Library	1	E232	3
Washington, DC 20361		R	1
		R10	1
Commander		R10A	1
U.S. Army Research and		R10A (K. Reed)	1
Development Command		R12	1
Attn: Technical Library	1	R12 (P. Walter)	2
Dover, NJ 07801		R13	1
		R13 (F. Zerilli)	2
Commander		R14 (K. Kiddy)	1
Air Force Weapons Laboratory		R14 (H. Mair)	1
Attn: Technical Library (SUL)	1	U	1
Kirtland AFB, NM 87117			
Commanding Officer			
Harry Diamond Laboratories			
Attn: Library	1		
2800 Powder Mill Road			
Adelphi, MD 20783			
Director			
Defense Research and			
Engineering			
Attn: Library	1		
Washington, DC 20305			
Lawrence Livermore National			
Laboratory			
Attn: Technical Library	1		
Livermore, CA 94550			
Los Alamos National Laboratory			
Attn: Technical Library	1		
P.O. Box 1663			
Los Alamos, NM 87544			
Library of Congress			
Attn: Gift and Exchange Division	4		
Washington, DC 20540			
Center for Naval Analyses			
4401 Fort Avenue			
P.O. Box 16268			
Alexandria, VA 22303-0268			

